OPEN ACCESS

University of BRISTOL

Luo, J., Macdonald, J., & Jiang, J. Z. (2017). Use of Inerter-based Vibration Absorbers for Suppressing Multiple Cable Modes. *Procedia Engineering*, *199*, 1695–1700. https://doi.org/10.1016/j.proeng.2017.09.370

Publisher's PDF, also known as Version of record

License (if available):
CC BY-NC-ND

Link to published version (if available):
10.1016/j.proeng.2017.09.370

Link to publication record in Explore Bristol Research
PDF-document

This is the final published version of the article (version of record). It first appeared online via Elsevier at https://doi.org/10.1016/j.proeng.2017.09.370. Please refer to any applicable terms of use of the publisher.

University of Bristol - Explore Bristol Research
General rights

This document is made available in accordance with publisher policies. Please cite only the published version using the reference above. Full terms of use are available:
http://www.bristol.ac.uk/red/research-policy/pure/user-guides/ebr-terms/

Available online at www.sciencedirect.com

ScienceDirect

Procedia Engineering 199 (2017) 1695–1700

Procedia Engineering

www.elsevier.com/locate/procedia

X International Conference on Structural Dynamics, EURODYN 2017

Use of Inerter-based Vibration Absorbers for Suppressing Multiple Cable Modes

Jiannan Luo, John H.G. Macdonald, Jason Zheng Jiang*

Faculty of Engineering, University of Bristol, Bristol, BS8 1TR, UK

Abstract

A common approach to the mitigation of vibrations of structural cables, e.g. on cable-stayed bridges, is to install a viscous damper transverse to the cable axis quite close to one end. The damping coefficient can be optimized for suppressing vibrations in one cable mode but the damper is then sub-optimal for other modes. This paper proposes the use of a passive inerter-based vibration absorber for suppressing multiple unwanted cable vibration modes. The inerter has the property that the force between its two terminals is proportional to their relative acceleration. A previous study has shown that inerter-based vibration absorber configurations can provide greater modal damping ratios than a viscous damper alone for vibration modes around the first undamped natural frequency. In this study, a finite-element model of a taut cable, together with a generic absorber is built. The absorber is located close to one end of the cable and represented by a general positive-real impedance function. The absorber layouts for maximizing the modal damping ratios over lower-frequency modes while perverting deterioration those for higher-frequency modes are identified. It will be shown that, compared with traditional viscous dampers, the proposed inerter-based vibration absorbers can give enhanced damping performance over multiple modes.

© 2017 The Authors. Published by Elsevier Ltd.
Peer-review under responsibility of the organizing committee of EURODYN 2017.

Keywords: Cable dynamics; vibration suppression; inerter; damper; mult-imode vibrations; optimisation.

1. Introduction

Stay cables are widely used in cable stayed bridges and other civil engineering structures in order to carry static loads, but they are often observed to experience large amplitude vibrations due to their low inherent damping ratio.

* Corresponding author. Tel.: 44 (0)117-95-45612.
E-mail address: z.jiang@bristol.ac.uk

1877-7058 © 2017 The Authors. Published by Elsevier Ltd.
Peer-review under responsibility of the organizing committee of EURODYN 2017.
10.1016/j.proeng.2017.09.370

Typically, the inherent damping ratio of bridge cables is of the order of 0.1% [1]. So, unless suppressed, these effects may cause severe vibrations, which could result in cable or connection failures due to fatigue, as well as damaging the corrosion protection system. Typically, only the first six modes with low natural frequencies are considered as they generally experience more significant vibrations than higher frequency modes [2].

Adding viscous dampers is a common method to suppress cable vibrations. It has been shown that the maximum possible damping ratio attainable in any specified mode is approximately 0.5 times the ratio of the damper's location and the total cable length [3]. However, the location of the damper is restricted to be near one end of the cable, generally up to 5% [4]. As a viscous damper alone is not very effective in suppressing vibrations in multiple modes, the potential of inerter-combined absorbers have been explored in a systematic manner to enhance the damping performance. The inerter was proposed as an ideal two terminal mechanical element, with the property that the applied force is proportional to the relative acceleration between its two terminals [5]. The inertance (the constant of proportionality, with dimensions of mass) can be much larger than the physical mass of the device due to gearing. Performance advantages of inerter combined dampers have been identified for road vehicles [6], railway vehicles [7], multi-story buildings [8], and also cables [9][10].

A previous study [10] identified inerter-combined absorbers which can improve the lowest frequency mode. It has then been found out that the beneficial absorbers will possibly lead deterioration to damping ratio for higher modes. This paper aims to maximize the damping ratio of the lowest frequency mode with the condition that damping ratios provided by modes 2-6 are no less than those of a viscous damper optimized for mode one. The results obtained will be more practical for industry applications. This paper is structured as follows. In Section 2, a finite element cable model with an admittance function representing a generic vibration absorber layout is recalled. All possible layouts with no more than one damper, one inerter and one spring each, as well as a proposed performance criterion, are then presented. In Section 3, the optimum performance of two-element and three-element layouts are analyzed and the corresponding parameter values are identified and compared. Conclusions are draw in Section 4.

2. Mathematical approach

In this section, a finite element model of a cable combined with an arbitrary linear passive absorber layout is introduced firstly. Then, a performance criterion representing low frequency damping performance and the optimization approach are introduced. Finally, the transfer functions of candidate absorber layouts are presented.

2.1. Mathematical model

Without considering minor effects such as cable's inclination, sag, out-of-plane motion and elasticity, a mathematical model of a cable with an absorber is introduced using the finite element method. The tension along the cable is denoted as T, the total mass of the cable is M, and the total length of the cable is L. Minor effects of the cable including inclination, sag, out-of-plane motion, and elasticity are neglected in the simplification. An example of a taut cable with n degree of freedom is shown in Figure 1. There are n masses of weight m spread along the cable and two masses of $m/2$ connected directly to the supports. Hence, $m = M/(n+1)$. These masses divide the cable into $n+1$ elements, each of length $l = L/(n+1)$. The a^{th} mass has an associated vertical position $x_a(t)$ simplified as x_a, which equals zero at equilibrium, and the relative displacements of mass a and mass $a+1$ leads to an angle θ_a. Since the masses at the end-points are connected directly to the supports, x_0 and x_{n+1} always equal zero.

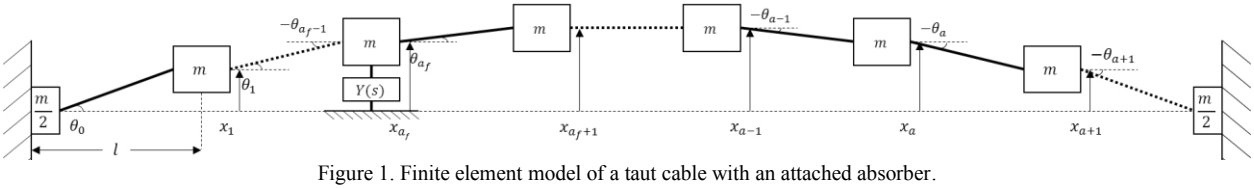

Figure 1. Finite element model of a taut cable with an attached absorber.

In designing the absorber, an estimate of the additional damping to be expected for the various modes of the cable is usually obtained by eigenvalue analysis. The equations of motion for each mass with no absorber attached and the

particular mass with additional force $F(t)$ provided by the absorber, are respectively shown by Equation (1a) and (1b). Where $\omega_o = \pi \cdot (T/ML)^{0.5}$ defined as the circular natural frequency of the first mode of the undamped cable.

$$\tfrac{1}{n+1}\ddot{x}_a = (n+1)\cdot(T/ML)\cdot(x_{a+1} - 2x_a + x_{a-1}) \,, \tag{1a}$$

$$\tfrac{1}{n+1}\ddot{x}_{a_f} = (n+1)\cdot(T/ML)\cdot\left(x_{a_f-1} - 2x_{a_f} + x_{a_f+1}\right) + \tfrac{F(t)}{M} \,. \tag{1b}$$

By arranging the displacements of the masses in the vector form, $\mathbf{x} = [x_1, x_2, x_3, \ldots, x_n]^{\mathrm{T}}$ and taking Laplace transforms, Equation (2) can be observed, where s is a complex number and tildes represent Laplace transforms.

$$\mathbf{M}s^2\tilde{\mathbf{x}} + \mathbf{C}s\tilde{\mathbf{x}} + \mathbf{K}\tilde{\mathbf{x}} = \mathbf{0} \,. \tag{2}$$

The elements in matrices $\mathbf{M}$, $\mathbf{C}$ and $\mathbf{K}$ are respectively described in Equations (3a) to (3c), in where δ_{ij} is the Kronecker delta function. $Y(s) = \tilde{F}(s)/[s\cdot\tilde{x}_{a_f}(s)]$ represents the admittance function of the absorber, which is defined as the ratio of force to velocity.

$$m_{ij} = \tfrac{1}{n+1}\delta_{ij} \,, \tag{3a}$$

$$c_{ij} = 0, \text{ except } c_{a_f a_f} = -Y(s)/M \,, \tag{3b}$$

$$k_{ij} = (n+1)\cdot(T/ML)\cdot(2\,\delta_{ij} - \delta_{i(j+1)} - \delta_{i(j-1)}) \,. \tag{3c}$$

The complex eigenvalues of Equation (2) can be calculated via Equation (4). The complex eigenvalues (represented by $[\boldsymbol{\lambda} \quad \boldsymbol{\lambda}^{*\mathbf{T}}]^{\mathbf{T}}$) of the system are calculated as roots of Equation (4), where $\boldsymbol{\lambda} = [\lambda_1,\ \lambda_2,\ \lambda_3,\ \ldots]$, $\mathbf{0}$ is the square null matrix of size n and $\mathbf{I}$ is the identity matrix of size n.

$$\det\left(\begin{bmatrix}\mathbf{0} & \mathbf{I}\\ -\mathbf{M}^{-1}\mathbf{K} & -\mathbf{M}^{-1}\mathbf{C}\end{bmatrix} - \begin{bmatrix}s\mathbf{I} & \mathbf{0}\\ \mathbf{0} & s\mathbf{I}\end{bmatrix}\right) = 0 \,. \tag{4}$$

The roots of Equation (4), represented by $[\boldsymbol{\lambda} \quad \boldsymbol{\lambda}^{*\mathrm{T}}]^{\mathrm{T}}$, are in complex conjugate pairs. The number of pairs is given by n plus the number of internal degree of freedom of the absorber. However, normally only a few pairs, representing low frequency modes, are of interest. Either eigenvalue λ_e (with positive imaginary part, $e = 1,2,3$ ...) or its complex conjugate eigenvalue $\lambda_e{}^*$ can be used to calculate the damping ratio ζ_e and the circular natural frequency ω_e of Mode e of the damped system, which are

$$\zeta_e = -\mathrm{Re}(\lambda_e)/\sqrt{\mathrm{Re}(\lambda_e)^2 + \mathrm{Im}(\lambda_e)^2} \,, \tag{5a}$$

$$\omega_e = \sqrt{\mathrm{Re}(\lambda_e)^2 + \mathrm{Im}(\lambda_e)^2} \,. \tag{5b}$$

2.2. Performance criteria and candidate absorber layouts

Modes with lower natural frequency are often more susceptible to vibrations. Since some candidate absorber layouts may introduce extra modes into the system, modes in the frequency range of $0\sim6.5\omega_o$ are analyzed in here to cover the first six modes of the undamped cable. The present study aims to maximize the critical damping ratio $\zeta_{c,opt}$, which is defined as the lowest damping ratio among all modes with natural frequencies in the range [0-$1.5\omega_o$). A constraint is implemented to guarantee that the damping ratios with natural frequencies in the range [$1.5\omega_o$-$6.5\omega_o$), are no less than those of a viscous damper optimized for mode one. For simplicity, the damping ratios for the viscous damper is represented by universal curve [4]. For a given inertance, the optimum $\zeta_{c,opt}$ is calculated by using the Matlab commands 'patternsearch' and 'fminsearch' respectively for fine-tuning of the parameters. Moveover, to balance the accuracy and the computational time a 19 DOF finite element model is used for the optimisations.

All absorber layouts with no more than one damper, inerter and spring each are considered as candidate layouts. For each layout, one terminal is connected to the cable at mass a_f and the other is attached to a fixed support. Because neither an inerter nor a spring can dissipate energy, a damper must be included in each candidate layout. Taken this

into consideration, there are in total four two-element and eight three-element absorber layouts that contain one damper. The admittance functions $Y(s)$ of all candidate absorber layouts are shown in Table 1. The network connections for each of the layouts can be worked out directly from corresponding admittance functions. For simplicity, these are not included.

Table 1. Admittance function $Y(s)$ for all candidate absorbers.

Layout	Admittance function	Layout	Admittance function
I	c	III-3	$1/[(1/bs)+(1/c)+(s/k)]$
II-1	$c+k/s$	III-4	$1/[1/(c+k/s)+(1/bs)]$
II-2	$1/[(1/c)+(s/k)]$	III-5	$1/[1/(c+bs)+(s/k)]$
II-3	$bs+c$	III-6	$1/[(1/bs)+(s/k)]+c$
II-4	$1/[(1/c)+(1/bs)]$	III-7	$1/[(s/k)+(1/c))]+bs$
III-1	$1/[(1/c)+(1/bs)]+(k/s)$	III-8	$bs+c+k/s$
III-2	$1/[1/(bs+k/s)+c]$		

The parameters of the absorber b, c and k represents inertance, damping coefficient and stiffness elements, respectively. For generality, they are presented in non-dimensional forms by using $b' = b/M$, $c' = (c/M)/(\omega_0/\pi)$ and $k' = (k/M)/(\omega_0/\pi)^2$. Similarly, non-dimensional frequency is defined as $\omega' = \omega_e/\omega_o$. Moreover, to make a fair comparison between candidate layouts, the relative location of all absorbers in this study is set to be 0.05 of the total length of the cable from one end.

3. Optimum performance of candidate absorber layouts

In this section, the optimum critical damping ratios for the four candidate layouts with two elements and the eight candidate layouts with three elements are studied. For Layouts II-1 and II-2, both the non-dimensional damping coefficient and non-dimensional stiffness are searched to optimize the critical damping ratio. For Layouts II-3, II-4 and III-1 to III-8, inerters with non-dimensional inertance b' ranging from 0 to 2.5 are considered as it covered the maximum optimum critical damping ratio for all layouts analyzed. From the optimized results for two element layouts, Layouts II-3, II-4 are considered beneficial as they can provide greater optimum critical damping ratios than that of a damper only. For three element layouts, Layout, III-4 and III-6 are considered beneficial, because compare with other three element layouts, they provide the largest optimum critical damping in certain inertance ranges. The beneficial absorber layouts with two or three elements are shown in Figure 2.

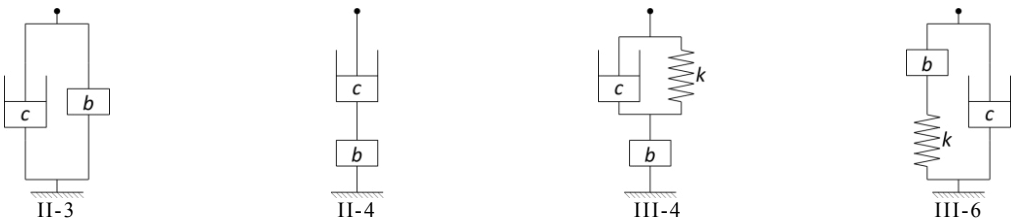

Figure 2. Beneficial absorber layouts with two (II-3, II-4) and three (III-4 III-6) elements.

3.1. Optimisation results for absorber layouts with two elements

Applying the optimisation criteria described in Section 2.2, the optimum critical damping ratios $\zeta_{c,opt}$ of both Layouts II-1 and II-2, are $\zeta_{c,opt} = 0.026$, which are the same as that of a damper only. The corresponding non-dimensional damping coefficient and stiffness are $c' = 6.43$, $k' = 0$ and $c' = 6.43$, $k' = \infty$ for Layouts II-1 and II-2 respectively (i.e. both without the spring). In fact, for any tested c', in the range 0 to 30, adding a spring always decreases the damping ratio for these two layouts. Therefore, these two layouts are not considered beneficial. Hence, only Layouts II-3 and II-4 are discussed below, together with a damper only. Their damping ratios and corresponding parameters are compared.

In Figure 3(a), the solid curve shows the optimum critical damping ratio for each b' according to performance criterion introduced in Section 2.2, including the condition for the higher mode in range [$1.5\omega_o$-$6.5\omega_o$), the results are same as in [10]. For comparison, the dashed curve shows the optimum critical damping ratio without considering higher modes, The lines in Figures 3(c), 4(a) and 4(b) are consistent in style with those used in Figure 3(a). According to Figure 3(a), with $b' = 0$, as expected, the optimised critical damping ratio is the same as that for a viscous damper only. For $b' > 0$, Layout II-3 provides a slightly greater optimum critical damping ratio than that for a viscous damper. It can be seen from the solid curve that among all the optimized results with varying b', the maximum optimum critical damping ratio $\zeta_{c,max}$ is 0.0283 for $b' = 0.160$. In Figure 3(b) the red solid curve illustrates the universal curve described in [4], which represents the lower boundary of the damping ratio for higher modes as in Section 2.2. And the crosses show the damping ratio of the first six modes when optimized for $b' = 0.170$. The damping ratio of mode six is the same as the lower limit of a damper only, which means at $b' = 0.170$ the optimized result for Layout II-3 is limited by mode 6. Therefore, the optimum critical damping ratio considering frequencies in the range [$1.5\omega_o$-$6.5\omega_o$), shown by blue curve in Fig 3 (a) is lower or equal to that without the higher modes, which shown by the dashed curve. When b' is greater than 0.185, the blue curve terminates since the damping ratio of mode 6 cannot reach the constraint that no worse than that for a viscous damper optimized for mode one.

Figure 3(c) shows the optimisation results for Layout II-4. The maximum optimum critical damping ratio $\zeta_{c,max}$ is 0.0622 for $b' = 2.172$, which is much greater than for a damper only. However, large inertance is required. The blue curve starts at $b' = 0.390$ since for small b' the damping ratio of mode 2 cannot reach the constraint. For $b' > 0.150$ the optimum solution is significantly limited by mode 6, giving greatly reduced result compared with the case without the additional constraint.

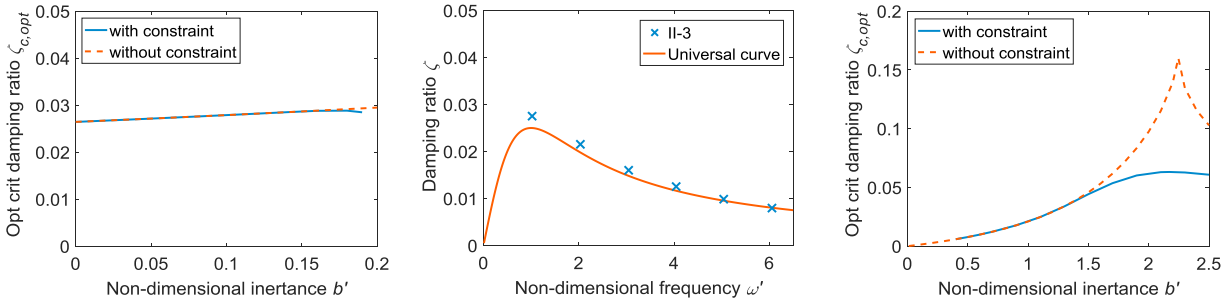

Figure 3. (a) Optimum critical damping ratio versus non-dimensional inertance for Layout II-3, (b) damping ratio limit for Layout II-3 when $b' = 0.170$, (c) optimum critical damping ratio versus non-dimensional inertance for Layout II-4.

3.2. Optimisation results for absorber layouts with three elements

There are eight possible absorber layouts with one element of each type, as shown in Table 1. Based on the optimization results, all candidate layouts can provide greater $\zeta_{c,opt}$ than layouts with fewer elements (Layout I, II-3 and II-4) with $0 \le b' \le 2.5$. However, layout III-6 and III-4 provides more beneficial optimised critical damping ratios than the rest. Therefore, their results are shown and discussed in detail.

Figure 4(a) shows the optimisation results for Layout III-4. The maximum optimum critical damping ratio $\zeta_{c,max}$ is 0.141 for $b' = 1.47$. The solid curve allowing the additional constraint starts at $b' = 0.390$ due to that the damping ratio of mode 2 cannot reach the condition that the damping ratio no less than for a viscous damper only optimized for mode one. For $b' \le 0.90$, the optimum solution is limited by mode 2 and for $b' > 1.40$ it is limited by mode 6. For $0.9 \le b' \le 1.4$, the result are not limited by the additional constraint, so the optimum solution is the same as when considering modes with frequencies in the range [$1.5\omega_o$-$6.5\omega_o$). For Figure 4(b) shows the optimisation results for Layout III-6. The maximum optimum critical damping ratio $\zeta_{c,max}$ is 0.032 for $b' = 0.224$. When $b' > 0.350$, due to its corresponding stiffness $k' = 0$ Layout III-6 performs the same as a damper only.

Figure 4(c) shows the optimisation results of all candidate absorber layouts considering b' ranging from 0 to 2.5. Layout III-6 in the range of $0 \le b' \le 0.52$ and III-6 in the range of $0.52 < b' \le 2.5$ provides more beneficial optimised critical damping ratios than the rest. Even though Layout III-4 provides the overall optimum critical

damping ratio, Layout III-6 is still worth considering in practice, because it provides reasonable benefits with relatively small inertance.

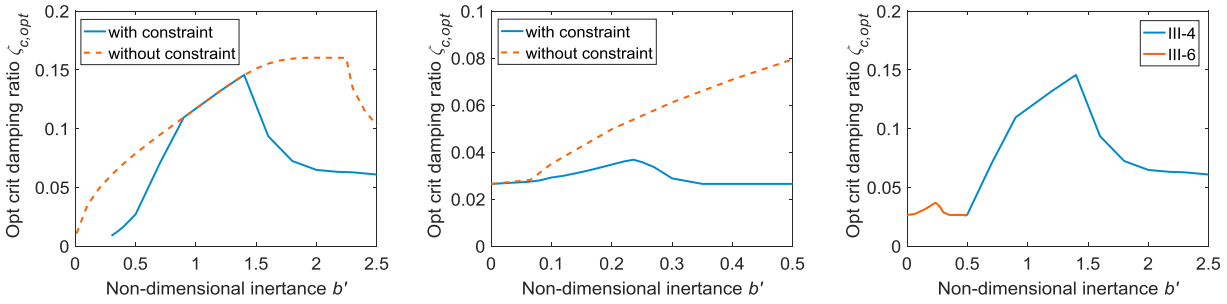

Figure 4. (a) Optimum critical damping ratio versus non-dimensional inertance for Layout III-4, (b) Layout III-6, (c) most beneficial layout among all candidate layouts.

4. Conclusion

In this paper, a Finite Element (FE) model of a cable with an absorber is recalled firstly. By using an admittance function to represent the absorber layout, a model of a cable with any passive linear absorber can be presented in the same form. Secondly, the performance criterion is established, which optimizes the damping ratio for mode(s) around the first natural frequency of the undamped cable, while keeping the damping ratio of modes up to the sixth mode no lower than that can be achieved by a viscous damper only. After that the performance of all possible absorber layouts with no more than one inerter, damper and spring each is analyzed and examined with non-dimensional inertance variable b' within a reasonable range of 0 to 2.5. Results show that all layouts with inerters included can provide more beneficial optimum critical damping ratio than a viscous damper only. However, there only are two layouts that give the most optimum results. They can provide much greater damping ratio than the other layouts in different inertance ranges, although their performance is often constrained by the additional criterion for mode 2 or 6.

Acknowledgements

The authors would like to acknowledge the support of the China Scholarship Council (CSC), by which Jiannan Luo is supported for his PhD study in the U.K.

References

[1] Yamaguchi H and Fujino Y, 1998. Stayed cable dynamics and its vibration control. Proceedings Int. Symposium on Advances in Bridge Aerodynamics, Balkema, Rotterdam, Netherlands, 235–253.
[2] Gimsing, N.J. and Georgakis, C.T., 2011. Cable supported bridges: concept and design third edition. John Wiley & Sons. London.
[3] Kovacs, I., Zur Frage der Seilschwingungen und der Seildampfung, Bautechnik, 10:325-332, 1982.
[4] Pacheco, B.M., Fujino, Y. and Sulekh, A., 1993. Estimation curve for modal damping in stay cables with viscous damper. Journal of Structural Engineering, 119(6):1961-1979.
[5] Smith M.C., 2002 Synthesis of mechanical networks: The inerter. IEEE Transactions on Automatic Control, 47 (10): 1648-1662.
[6] Smith, M.C. and Wang, F.C., 2004. Performance benefits in passive vehicle suspensions employing inerters. Vehicle System Dynamics, 42(4):235-257.
[7] Jiang, J.Z., Matamoros-Sanchez, A.Z., Goodall, R.M. and Smith, M.C., 2012. Passive suspensions incorporating inerters for railway vehicles. Vehicle System Dynamics, 50(sup1):263-276.
[8] Zhang, Y., Jiang, J.Z. and Neild, S.A., 2016. Optimal Configurations for a Linear Vibration Suppression Device. in a Multi-Storey Building. Structural Control and Health Monitoring, doi: 10.1002/stc.1887.
[9] Lazar, I.F., Neild, S.A. and Wagg, D.J., 2016. Vibration suppression of cables using tuned inerter dampers. Engineering Structures, 122:62-71.
[10] Luo, J., Jiang, J.Z., & Macdonald, J.H.G., 2016. Vibration Suppression of Stay Cables Using Absorbers Incorporating Inerters. in: Thirteenth International Conference on Motion and Vibration Control (MOVIC 2016, Southampton, UK.)